Strategies for Functional Validation of Genes Involved in Reproductive Stages of Orchids[1]

Hsiang-Chia Lu, Hong-Hwa Chen, Wen-Chieh Tsai[2], Wen-Huei Chen, Hong-Ji Su, Doris Chi-Ning Chang, and Hsin-Hung Yeh*

Department of Plant Pathology and Microbiology (H.-C.L., J.-J.S., H.-H.Y.) and Department of Horticulture (D.C.-N.C.), National Taiwan University, Taipei 106, Taiwan; Department of Life Sciences (H.-H.C., W.-C.T.) and Institute of Biotechnology (H.-H.C.), National Cheng Kung University, Tainan 701, Taiwan; and Department of Life Sciences, National University of Kaohsiung, Kaohsiung 811, Taiwan (W.-H.C.)

Plants in the largest family of angiosperms, Orchidaceae, are diverse in both specialized pollination and ecological strategies and provide a rich source for investigating evolutionary relationships and developmental biology. However, studies in orchids have been hindered by several challenges that include low transformation efficiency and long regeneration time. To overcome such obstacles, we selected a symptomless cymbidium mosaic virus (CymMV) isolate for constructing virus-induced gene-silencing vectors. The feasibility of the virus vectors was first assessed with use of an orchid phytoene desaturase gene. The vector was able to induce gene silencing in orchids; however, because of the slow growth of orchids, the commonly used phytoene desaturase gene was not a good visual marker in orchids. We inserted a 150-nucleotide unique region of a B-class MADS-box family gene, *PeMADS6*, into pCymMV-pro60. The transcription level of *PeMADS6* in inoculated Phalaenopsis plants was reduced by up to 73%, but no effect was observed for other MADS-box family genes. In contrast, in Phalaenopsis plants inoculated with CymMV transcripts containing 500 nucleotides of *PeMADS6*, a conserved region among MADS-box genes, the transcription level of *PeMADS6* and the B- and C-class MADS-box genes was reduced by up to 97.8% as compared with plants inoculated with the vector alone. Flower morphology was affected in the MADS-box family gene-silenced plants as well. This in vivo experiment demonstrates an efficient way to study genes involved in the reproductive stage of plants with a long life cycle.

Functional genomics studies of nonmodel organisms to reveal how changes in regulatory networks contribute to diversity have been a big challenge in biology (Pennisi, 2004; Costa et al., 2005; Gewin, 2005). Studies of nonmodel organisms may be hindered by their large genome size, low transformation efficiency and long regeneration time, and long life cycle. Advances in sequencing technology have alleviated the difficulties in obtaining genetic information from organisms with large genome size. For example, construction of an expressed sequence tag (EST) database can reveal a massive amount of genetic information reflecting an important biological state in a short period. However, this information needs further analysis to define its biological significance. Most gene function validation approaches require extensive genetic screening and plant transformation. Likewise, these approaches are suitable for model plants, but are not practical for plants with low transformation efficiency, long regeneration time, and long life cycle. In particular, a formidable obstacle rests in functional genomics studies of genes involved in the final stage of the life cycle, the reproductive stage, in plants with long life cycles. For such plants, years may be required to obtain data by conventional approaches to study genes involved in the reproductive stage. Unfortunately, the life cycles of most plants are longer than 1 year.

The family of Orchidaceae has an estimated population of more than 35,000 species and is among the largest families of the flowering plants (Dressler, 1993). The family is known for its diversity of both specialized pollination and ecological strategies and so provides a rich subject for investigating evolutionary relationships and developmental biology. The versatility and specialization of orchid floral morphology, structure, and physiological properties have fascinated botanists and collectors for centuries. The most astonishing evolution is seen in reproductive biology. Yet, popular orchids, such as *Phalaenopsis* spp., have a large genome size, ranging from 1×10^9 to 6×10^9 bp/1 C (Chen et al., 2001; Lin et al., 2001) and several important commercial cultivars are multiploid. The life cycle of *Phalaenopsis* spp. naturally takes about 2 to 3 years for the transition from the vegetative phase to the reproductive phase.

A recent alternative approach to plant loss-of-function assay is virus-induced gene silencing (VIGS). The mechanism and advantage of VIGS has been widely reviewed (Marathe et al., 2000; Benedito et al., 2004; Burch-Smith

[1] This work was supported by the Council of Agriculture, Taiwan (grant no. 91–agriculture–3.1.3–food–Z3), and the National Science Council, Taiwan (grant nos. NSC 92–2317–B–002–022, NSC 93–2317–B–002–013, NSC 94–2317–B–002–007, and NSC 95–2317–B–002–006).

[2] Present address: Department of Biological Science and Technology, Chung Hwa College of Medical Technology, Tainan County 717, Taiwan.

* Corresponding author; e-mail hyeh@ntu.edu.tw; fax 886–2–23636490.

The author responsible for distribution of materials integral to the findings presented in this article in accordance with the policy described in the Instructions for Authors (www.plantphysiol.org) is: Hsin-Hung Yeh (hyeh@ntu.edu.tw).

www.plantphysiol.org/cgi/doi/10.1104/pp.106.092742

et al., 2004, 2006; Robertson, 2004). Compared with transforming plants with sense and/or antisense genes, VIGS is much faster. Moreover, VIGS can suppress the RNA level of a target gene after seedlings are established and thus it prevents suppression of some essential genes required for development. Because of the host range limitation of the currently constructed virus vectors, application of VIGS is restricted to plants such as tomato (*Lycopersicon esculentum*), Arabidopsis (*Arabidopsis thaliana*), and tobacco (*Nicotiana benthamiana*; Wang and Waterhouse, 2002; Benedito et al., 2004; Burch-Smith et al., 2004; Valentine et al., 2004; Katou et al., 2005). Recent efforts have extended the host ranges of VIGS vectors in some *Solanum* spp; a legume species, pea (*Pisum sativum*); soybean (*Glycine* spp.); and poppy (*Papaver somniferum*; Brigneti et al., 2004; Constantin et al., 2004; Fofana et al., 2004; Hileman et al., 2005; Zhang and Ghabrial, 2006). Among monocots, so far only a barley (*Hordeum vulgare*) strip mosaic virus-derived vector has been developed for VIGS (Holzberg et al., 2002; Scofield et al., 2005). More virus vectors are urgently needed for speeding up the characterization of gene functions of important nonmodel plants.

Recently, a floral EST database of *Phalaenopsis equestris* was established with thousands of unigenes, including five MADS-box genes, identified (Tsai et al., 2004, 2005, 2006). From the available sequence information, we attempted to investigate nonmodel plants, such as *Phalaenopsis* spp. We first selected a symptomless *Cymbidium mosaic virus* (CymMV), one of the most prevalent orchid viruses, to develop vectors for identification of gene functions of orchids. In addition, we developed a strategy combining data from the EST library with simple physiological controls and VIGS. The success of our strategy was verified by functional validation of floral identity genes in the tetraploid Phalaenopsis orchids, which have an unusually long life cycle (2 years from sowing to flowering). We could knock down the RNA level of either a specific floral identity gene or, congruently, floral identity family genes in Phalaenopsis in less than 2 months. Expected and unexpected morphological changes were observed in floral identity family gene-silenced plants. Because CymMV has a wide host range among Orchidaceae, we believe that the use of constructed CymMV-based vectors or similar approaches will be beneficial in orchid functional genomics studies. Moreover, the developed strategies will contribute well to functional genomics studies of plants for which general conventional molecular and genetic approaches are not available.

RESULTS

Construction of CymMV cDNA Infectious Clones

To avoid symptoms and physiological change induced by CymMV infection that may complicate VIGS results, we selected a mild, symptomless CymMV strain isolated from *Phalaenopsis* spp. (see ''Materials and Methods'') to construct a cDNA infectious clone. The pCymMV-M1 infectious clone contains a T3 promoter immediately adjacent to the 5′ end of CymMV and a poly(A) tail (25 adenosines) followed by an *Spe*I site immediately downstream of the CymMV 3′ end (Fig. 1A). No symptoms were observed on pCymMV-inoculated plants even 6 months after inoculation (Fig. 2A). To compare the infection between the

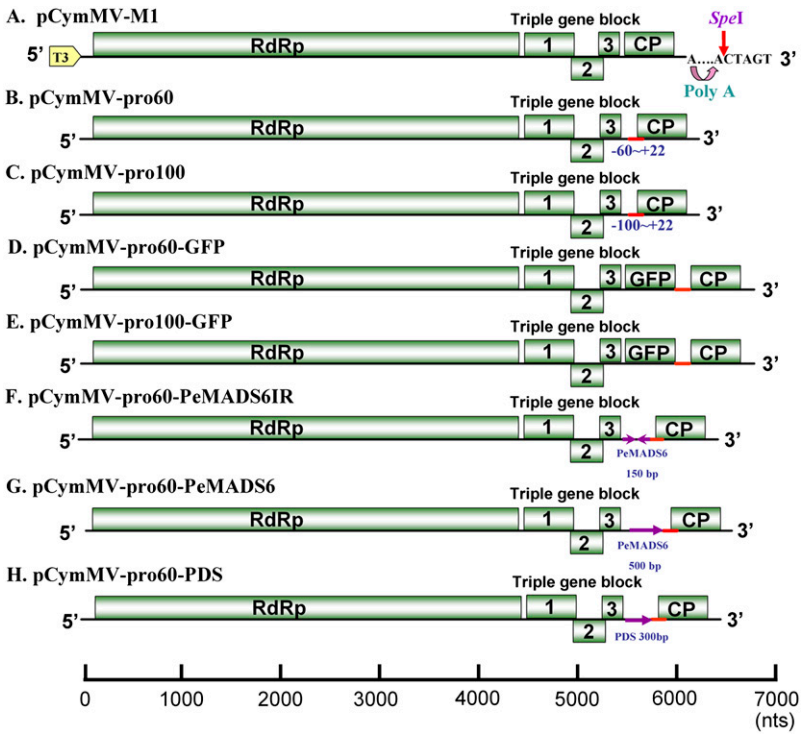

Figure 1. Schematic representation of CymMV cDNA infectious clone (A) and derivative vectors (B–H). Rectangles represent open reading frames encoded by CymMV genomic RNA. RNA-dependent RNA polymerase (RdRp), triple gene block 1, 2, and 3, CP, and GFP are indicated. The T3 promoter immediately adjacent to the most 5′ end and a poly(A) tail (25 adenosine) at the most 3′ end is indicated. The *Spe*I restriction enzyme digestion site is indicated by an arrow. The numbers below the red lines indicate the selected region of the CP subgenomic promoter; plus or minus corresponds to the upstream and downstream CP translation start codon, respectively. Head-to-head arrows on F indicate that the selected 150 bp of *PeMADS6* was cloned as an inverted repeat. The direct arrows on G and H indicate that the *PeMADS6* and PDS gene conserved regions were cloned directly. Scale bar, in nucleotides, is shown at the bottom.

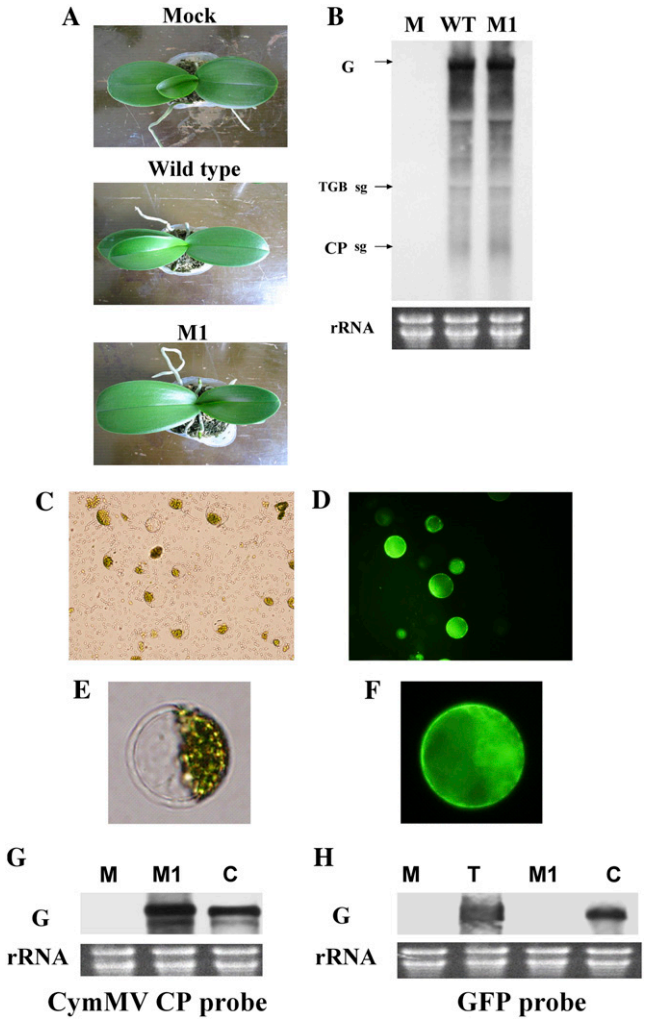

Figure 2. Symptoms and infectivity assay of CymMV infectious clones (A) and detection of CymMV in infected leaves by northern-blot hybridization (B). *P. amabilis* var. *formosa* infected with buffer (Mock), sap extracted from the symptomless CymMV-infected plants (wild type), and transcripts derived from pCymMV-M1 (M1). Photos were taken 6 months postinoculation. Total nucleic acids were extracted from CymMV-infected systemic leaves and underwent northern-blot hybridization with DIG-labeled minus sense probes corresponding to the CymMV 3′ end 590 nucleotide. Nucleic acids purified from mock-inoculated plants (lane M), CymMV wild-type inoculated plants (WT), or transcripts of pCymMV-M1-inoculated plants (M1). Genomic RNA (G), triple gene-block subgenomic RNA (TGB sg), and CP subgenomic RNA (CP sg) are indicated. Ribosomal RNA (rRNA) used for loading control is also indicated. CP subgenomic promoter assay (C–F). The subgenomic promoters (see "Materials and Methods") were inserted in the CymMV 5,502 nucleotide for CP expression (Fig. 1A). Foreign genes can be expressed through subgenomic RNA derived from the CP subgenomic promoter. GFP was introduced in pCymMV-pro60 to construct the plasmid for pCymMV-pro60-GFP. A total of 5×10^5 tobacco protoplasts were inoculated with the transcripts of pCymMV-CP60-GFP. Cells were examined 24 h postinoculation by light (C and E) and fluorescent microscopy (D and F). Stability of foreign genes in pCymMV-pro60 (G and H) northern-blot hybridization was performed with a DIG-labeled minus-sense probe corresponding to the CymMV 3′ end 590 nucleotide (G) and the GFP 3′ end 533 nucleotide (H). Total nucleic acids were purified from mock-inoculated plants (M) and plants inoculated with the same amount of transcripts derived from pCymMV-M1 (M1) and pCymMV-pro60-GFP (C). Genomic RNA (G) and ribosomal rRNA are indicated. Transcripts derived from pTMV-GFP30B (contain GFP; T; Shivprasad et al., 1999) were used as a GFP hybridization positive control.

wild-type virus and the derived cDNA infectious clone, sap extracted from plants infected with wild-type virus and transcripts of pCymMV-1 were used to inoculate *Phalaenopsis amabilis* var. *formosa*. Northern-blot analysis detected CymMV in systemic leaves 14 d postinoculation and similar amounts of viral RNA were detected in plants infected with wild-type virus or pCymMV-M1 (Fig. 2B).

Construction of VIGS Vectors

To highly transcribe foreign RNA, we duplicated a subgenomic promoter of coat protein (CP) to construct the CymMV vector (Chapman et al., 1992). The duplicated promoters were inserted in the CymMV 5,502 nucleotide for CP expression (Fig. 1, B–H). Foreign genes were expressed through subgenomic RNA derived from the original CP subgenomic promoter (Fig. 1, B–H). Two expression vectors with differences in lengths of the duplicated subgenomic promoters were constructed and named pCymMV-pro60 and pCymMV-pro100, respectively (Fig. 1, B and C). Green fluorescent protein (GFP) was introduced to construct the plasmids pCymMV-pro60-GFP and pCymMV-pro100-GFP (Fig. 1, D and E). To test the expression of these vectors, transcripts derived from each vector were inoculated into tobacco protoplasts (a natural host of our selected CymMV isolate). About 20% to 28% of protoplasts emitted fluorescence 14 h postinoculation (Fig. 2, D and F). The same amount of transcripts from pCymMV-M1, pCymMV-pro60-GFP, and pCymMV-pro100-GFP was used to inoculate leaves of *P. amabilis* var. *formosa*; both transcripts systemically infected entire plants and were detected 28 d postinoculation (Fig. 2, G and H). Thus, both the selected CP subgenomic promoters were functional and the expression vectors could maintain the foreign gene even at 28 d postinoculation. Because a longer fragment of duplicated promoters in the virus vector may have a higher chance for recombination, either as plasmids propagated in *Escherichia coli* or as RNA viruses in plants, we used pCymMV-pro60 in the following experiments.

Validation of the CymMV Vector in Inducing Gene Silencing

The feasibility of virus vectors to induce gene silencing was first assessed with the use of an orchid phytoene desaturase (PDS) gene. PDS is a visual marker commonly used for VIGS because the bleaching phenotype is easily observed on newly emerging leaves (Kumagai et al., 1995; Ruiz et al., 1998; Ratcliff et al., 2001).

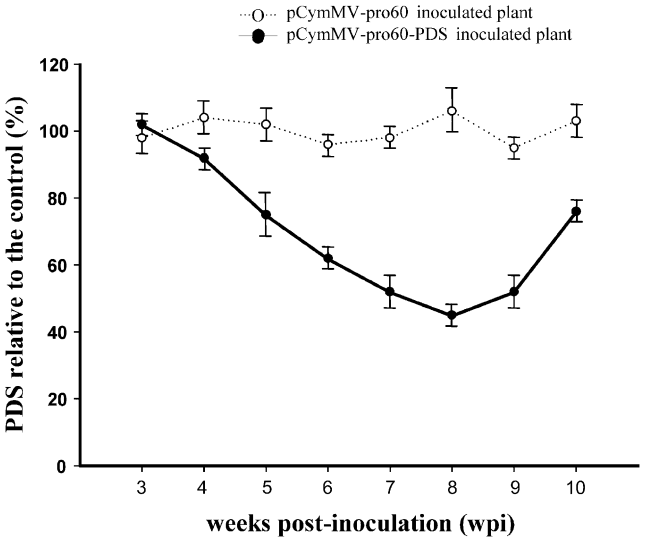

Figure 3. Relative quantification of the PDS gene in inoculated *P. amabilis* var. *formosa* by real-time RT-PCR. Mean PDS transcript level in mock-inoculated plants set to 100% for relative quantification. The calculation is based on two individual experiments. In each experiment, 12 plants were used for each treatment and three randomly selected plants were used in each quantification.

P. amabilis PDS was amplified and cloned to pCymMV-pro60 to construct pCymMV-pro60-PDS and derived transcripts were used to inoculate *P. amabilis.* To monitor the knockdown effect induced by pCymMV-pro60-PDS, real-time reverse transcription (RT)-PCR was used to quantify the level of PDS RNA at 3 weeks (3 weeks are needed for CymMV to establish systemic infection) after inoculation (Fig. 3). The RNA level of PDS was gradually reduced in pCymMV-pro60-PDS-inoculated plants to 54% at 8 weeks postinoculation, with the level increasing thereafter; thus, gene-silencing efficacy was reduced after 8 weeks (Fig. 3). However, we did not observe white-colored leaves on the inoculated orchids because Phalaenopsis is a Crassulacean acid metabolism plant with a very slow growth rate and no new leaves emerged over such a short time. Thus, we concluded that the developed vector could induce gene silencing in orchids, but the commonly used PDS gene was not a good visual marker in orchids.

Validation of the CymMV Vector in Inducing Floral Gene Silencing

For orchid gene functional validation, the most intriguing and challenging studies are analyzing genes involved in reproductive stages. To test whether the vector could induce floral gene silencing in orchids, we analyzed an orchid floral organ identity *GLOBOSA/PISTILLATA*-like gene, *PeMADS6* (a B-class MADS-box gene), which is transcribed in all floral organs (Tsai et al., 2004, 2005). To specifically knock down *PeMADS6*, we amplified a 150-bp fragment at the 3′ end of *PeMADS6* (Fig. 4). Because inverted repeat sequences can enhance gene silencing (Smith et al., 2000; Wesley et al., 2001), we cloned the 150-bp fragment into the pCymMV-pro60 as an inverted repeat and named the result pCymMV-pro60-PeMADS6-IR (Fig. 1F).

To test VIGS induction ability in different Phalaenopsis orchids, we analyzed a Taiwanese native species, *P. amabilis* var. *formosa*, and a commercial cultivar, *Phalaenopsis* Sogo Musadium. Plants were first subjected to low-temperature controls (25°C/d and 20°C/night) with appropriate humidity and fertilization to induce stalks for flowering (Gorden, 1998). This process has been commonly applied in most orchid nurseries to produce flowers year round and is advantageous for more frequent study.

Emerging stalks with six nodes (about 8 cm) were inoculated with pCymMV-pro60 and pCymMV-pro60-PeMADS6-IR. Approximately 6 weeks later, flowers blossomed. Real-time RT-PCR was performed to assess the relative transcription level of *PeMADS6* in sepals, petals, lips, and columns of inoculated plants. Compared to mock-inoculated plants, plants inoculated with pCymMV-pro60-PeMADS6-IR showed reduced levels of *PeMADS6* RNA in sepals, petals, lips, and columns—63% ± 2%, 33% ± 3%, 23% ± 5%, and 33% ± 2%, respectively, in *P. amabilis* var. *formosa* (Fig. 5A) and 73.5% ± 6.5%, 55% ± 3%, 32% ± 1%, and 80% ± 10%, respectively, in *P.* Sogo Musadium (Fig. 5B). Mock- and pCymMV-pro60-inoculated plants showed similarly high *PeMADS6* RNA levels. We also analyzed the RNA level of two randomly selected MADS-box family genes, *PeMADS1* and *PeMADS3*, belonging to the C and B classes, respectively, in inoculated plants, with no transcriptional changes detected for either in plants inoculated with buffer, pCymMV-pro60, or pCymMV-pro60-PeMADS6-IR (data not shown). Thus, the knockdown of *PeMADS6* in plants inoculated with pCymMV-pro60-PeMADS6-IR was specific.

We noticed fairly wide variation in gene silencing in floral tissues, which could have been related to different background levels of the target gene or differential replication/expression efficiency of CymMV per se. To differentiate between these two possibilities, we used real-time RT-PCR to determine the RNA level of *PeMADS6* and CymMV (Fig. 5). The differential silencing of *PeMADS6* in various floral organs was related more to the accumulation of CymMV (Fig. 5C) than to the endogenous differential transcription levels of *PeMADS6* (Fig. 5D).

To confirm that reduced expression of *PeMADS6* RNA was due to RNA interference caused by VIGS, low-molecular-weight RNA was purified from *P. amabilis* var. *formosa* inoculated with pCymMV-pro60 (Fig. 6, A and B, lane 2) and pCymMV-pro60-PeMADS6-IR (Fig. 6, A and B, lane 3) and subjected to northern-blot hybridization with CymMV CP (Fig. 6A) and *PeMADS6* probes (Fig. 6B). Virus-induced small interfering (si) RNA was detected in plants inoculated with both pCymMV-pro60 and pCymMV-pro60-PeMADS6-IR with CymMV CP used as a probe (Fig. 6A, lanes 2 and 3). In contrast, virus-induced siRNA was detected only in plants inoculated with pCymMV-pro60-PeMADS6-IR with *PeMADS6* used as a probe (Fig. 6B,

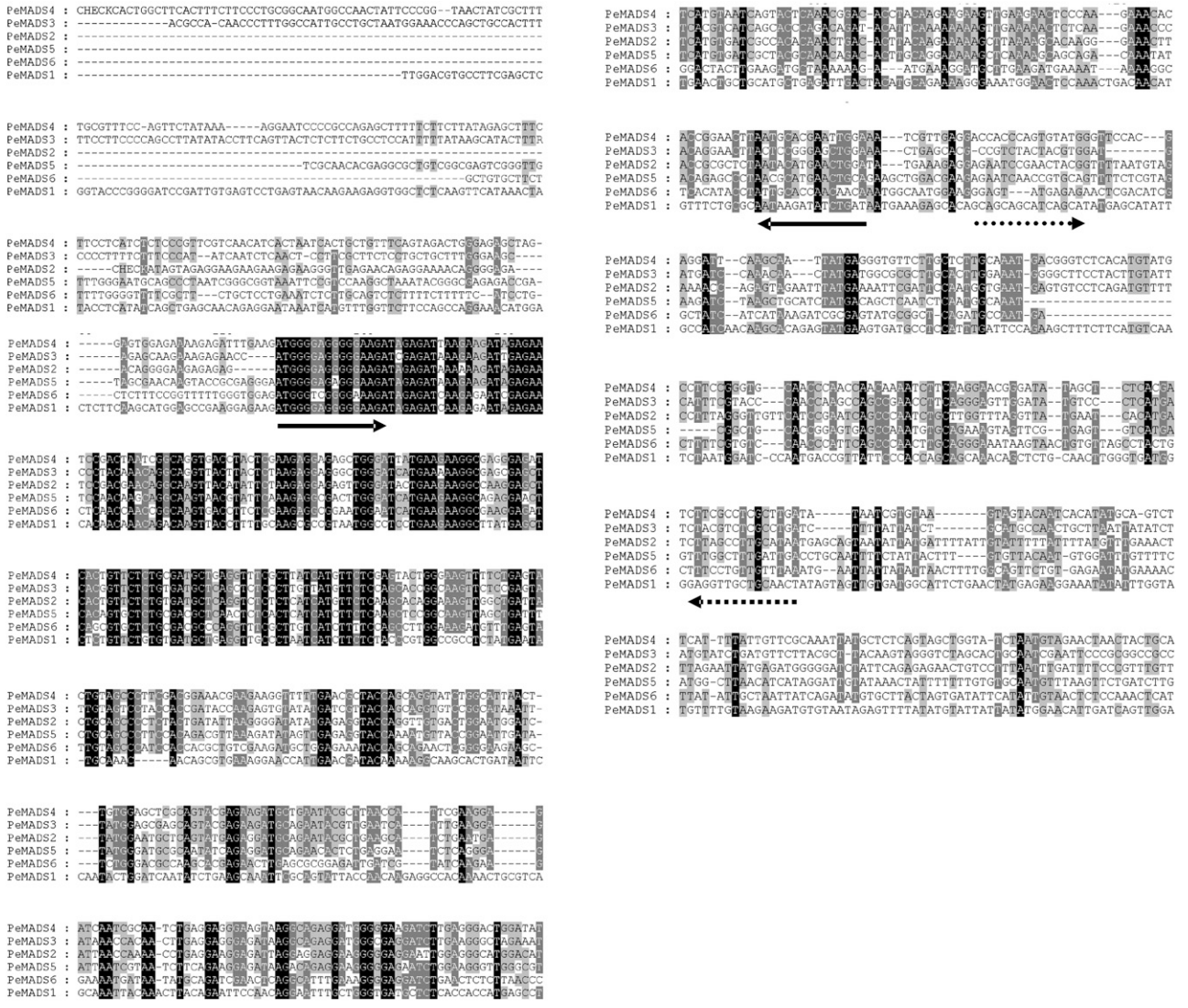

Figure 4. Sequence alignment of the MADS-box gene family identified in *P. equestris*. The MADS-box genes identified in *P. equestris* (*PeMADS 1–6*) were aligned by use of ClustalW 1.8. Primers used for amplifying the *PeMADS6* specific and conserved regions to insert in pCymMV-pro60 are indicated by discontinuous and solid arrows, respectively.

lane 3). With either probe, siRNA was not detected in mock-inoculated plants (Fig. 6, A and B, lane 1). Similar siRNA findings were detected in *P.* Sogo Musadium (data not shown). These results indicated that the CymMV VIGS vector induced *PeMADS6* siRNA only when the specific sequence of *PeMADS6* was inserted in the CymMV vector, which suggests that reduced *PeMADS6* expression was indeed mediated via the gene-silencing mechanism (Shivprasad et al., 1999). However, no obvious visible morphological changes were observed in *PeMADS6*-silenced plants.

Simultaneous Knock Down of MADS-Box Genes

Family genes with redundant functions are not easily targeted by genetic knockout assay. In addition, a vector that can easily induce a visible phenotype in orchids during VIGS will be desirable for further research. Therefore, we tried to knock down floral MADS-box genes simultaneously by inserting a 500-bp DNA fragment of *PeMADS6* containing a conserved region of the MADS-box genes into pCymMV-pro60l; the resulting plasmid was named pCymMV-pro60-PeMADS6 (Figs. 1G and 4). We expected that several MADS-box genes would be affected, with consequent prominent morphological changes.

Approximately 2 months postinoculation, flowers blossomed; but streaks or patches of greenish tissues were observed in sepals, petals, and lips of flowers of *P. amabilis* and *P.* Sogo Musadium inoculated with pCymMV-pro60-PeMADS6 (Table II; Fig. 7, A–I). The greenish tissues were more prominent in the abaxial than adaxial side. The more detailed morphological

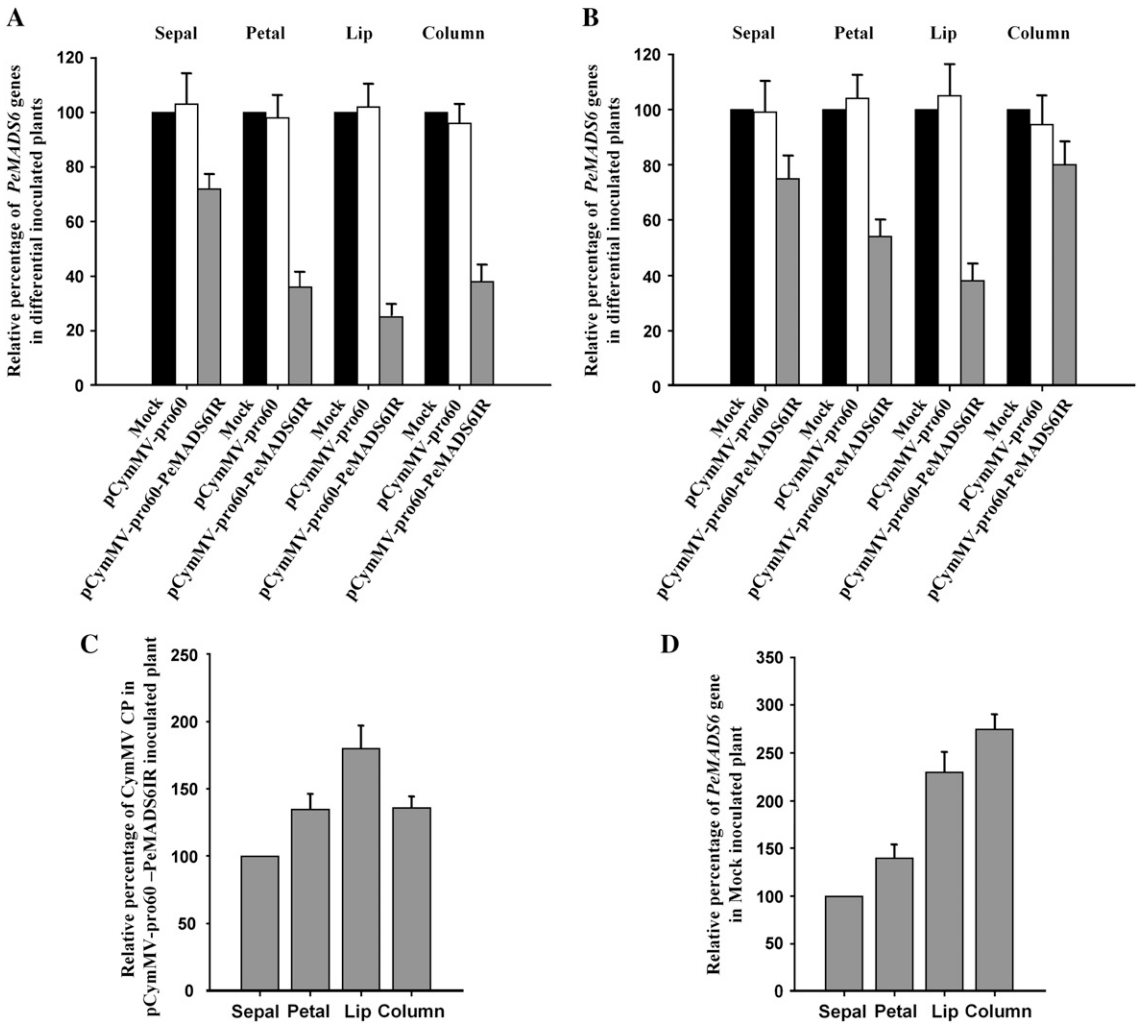

Figure 5. Relative quantification of *PeMADS6* and CymMV by real-time RT-PCR. Relative quantification of *PeMADS6* in *P. amabilis* var. *formosa* (A) or *P.* Sogo Musadium (B) infected with buffer (mock), pCymMV-pro60, or pCymMV-pro60-PeMADS6IR. A and B, Mean *PeMADS6* transcript level of plants inoculated with buffer was set to 100%. C, Mean CymMV RNA level of sepals of *P. amabilis* var. *formosa* inoculated with pCymMV-pro60 was set to 100%. D, Mean *PeMADS6* transcript level of sepals of *P.* Sogo Musadium was set to 100%. The calculation is based on three and two individual experiments for *P. amabilis* var. *formosa* and *P.* Sogo Musadium, respectively. In each experiment, six plants were used in each treatment and three randomly selected plants were used for quantification.

changes are listed in Table II. All these phenotypes were observed in both varieties (Tables I and II), except that the greenish streaks were more prominent in sepals and petals of *P.* Sogo Musadium (Fig. 7, A–C).

Scanning electron microscopy revealed that the greenish tissues on the adaxial or abaxial side of the petal epidermis of inoculated plants could not form conical cells (Fig. 8, E and F), a typical cell type of the petal. In addition, the adaxial side of the lip epidermis of inoculated plants could not form cuticular striations (Fig. 8, D and H). In contrast, the floral morphology was similar between plants of *P.* Sogo Musadium inoculated with buffer or pCymMV-pro60.

To analyze whether different MADS-box genes were silenced simultaneously in buds and flowers of plants inoculated with pCymMV-pro60-MADS6, we compared the transcription levels of three MADS-box genes, *PeMADS3* and *PeMADS6* (B class like) and *PeMADS1* (C class like), by real-time RT-PCR. *PeMADS1*, *PeMADS3*, and *PeMADS6* were all silenced in plants inoculated with transcripts derived from pCymMV-pro60-PeMADS6 (Fig. 9). In addition, the transcript level of all analyzed genes was similar in both mock- and pCymMV-pro60-inoculated plants (data not shown).

Interestingly, some *P. amabilis* and *P.* Sogo Musadium inoculated with pCymMV-pro60-PeMADS6 initially produced flower buds on the lower stalks, but the buds were unable to blossom (Table II). The flower buds on the upper stalk were able to blossom to some extent; however, streaks or patches of greenish tissues were observed in sepals, petals, and lips. We dissected

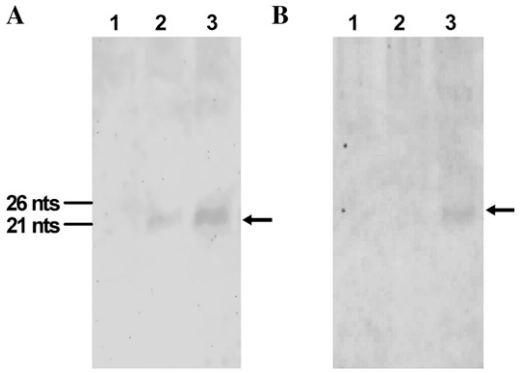

Figure 6. Detection of siRNA. siRNA was detected by northern-blot hybridization with a DIG-labeled minus-sense RNA probe corresponding to the CymMV CP 3′ end 590 nucleotide (A) or DNA probes corresponding to full-length *PeMADS6* (B). Low-molecular-weight nucleic acids purified from plants inoculated with mock (lane 1) transcripts or pCymMV-pro60 (lane 2) or pCymMV-pro60-PeMADS6-IR (lane 3) were used for analysis.

some initial flower buds that turned yellow (an indication that these buds would eventually abort) and found fully formed sepals, petals, lips, and columns within the buds and morphology similar to that of green buds of healthy plants (data not shown). These results suggest that the reduced transcript level of MADS-box family genes still allowed the flower to develop normally initially, but not enough for the flower to further develop and blossom in these plants.

Because VIGS efficacy was progressively reduced over time and the initial buds of plants inoculated with pCymMV-pro60-MADS6 were unable to blossom, we speculated that gene silencing was more effective in the initial flower buds than in the later blossomed flowers. Therefore, we collected initial green buds with similar size (2 cm in diameter) from mock-, pCymMV-pro60-, and pCymMV-pro60-PeMADS6-inoculated plants. Results of real-time RT-PCR revealed reduced RNA levels more prominent in flower buds than in later blossomed flowers (Fig. 9); for *PeMADS1*, *PeMADS3*, and *PeMADS6*, more than 85% of the transcript level was reduced in the initial flower buds (Fig. 9A).

DISCUSSION

In this study, we established a new CymMV-based VIGS vector. Because CymMV has a wide host range among species belonging to Orchidaceae, the vector will be an important tool for the study of the largest family of flowering plants. In addition, we also developed strategies that could easily be used to knock down genes involved in the reproductive stages of plants with long life cycles. Because the life cycle of most plants is more than 1 year, we foresee that studies of genetics, evolution, and development in planta will

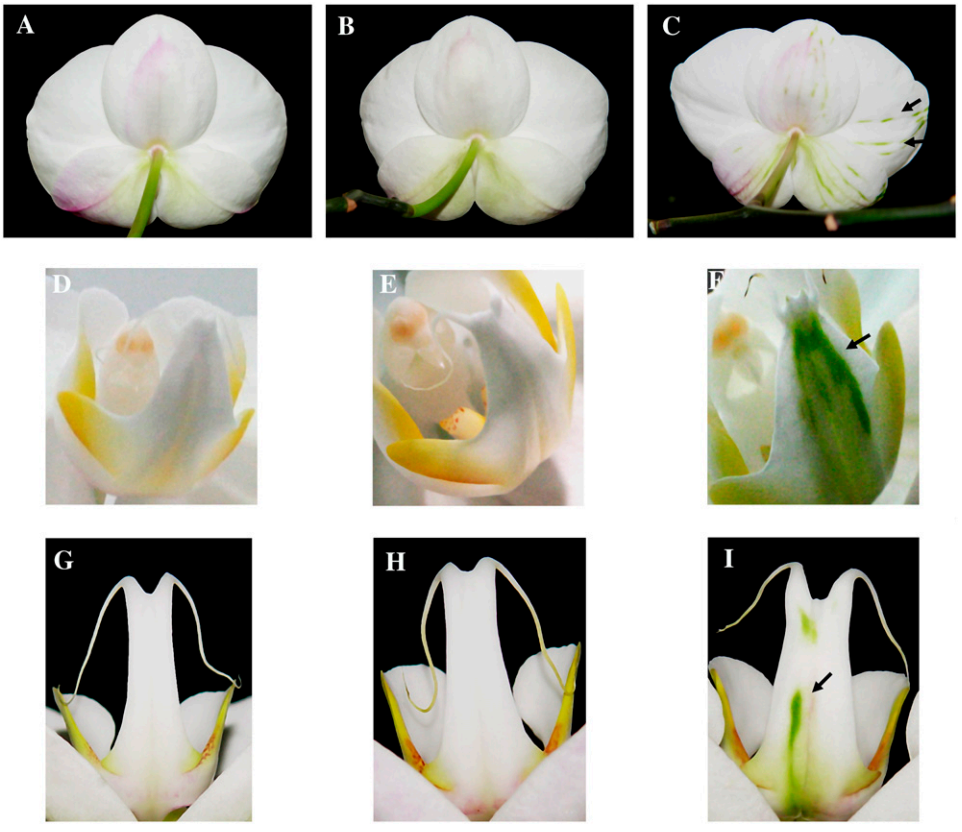

Figure 7. Phenotype on MADS-box gene-silenced plants. Plants were infected with buffer (A, D, and G), pCymMV-pro60 (B, E, and H), or pCymMV-CP60-PeMADS6 (C, F, and I). D to F, *P. amabilis* var. *Formosa*. A to C and G to I, *P.* Sogo Musadium. The arrows on C indicate greenish streaks of the flower and those on F and I indicate greenish patches of the lip.

Table I. *Ratio of infectivity and morphological change in inoculated Phalaenopsis orchids*

	Mock	pCymMV-pro60	pCymMV-pro60-PeMADS6
P. amabilis var. *formosa*			
Exp. 1			
Infectivity	0/6[a]	6/6	8/8
Morphological change	0/6[b]	0/6	8/8
Exp. 2			
Infectivity	0/4	4/4	6/6
Morphological change	0/4	0/4	5/6
Exp. 3			
Infectivity	0/6	6/6	8/8
Morphological change	0/6	0/6	7/8
P. Sogo Musadium			
Exp. 1			
Infectivity	0/3	3/3	3/3
Morphological change	0/3	0/3	3/3
Exp. 2			
Infectivity	0/4	4/4	6/6
Morphological change	0/4	0/4	5/6

[a]Number of infected plants (Exp.) to total number of inoculated plants. [b]Number of plants with morphological change to total number of inoculated plants.

be greatly promoted by the strategies we describe here (Babbitt et al., 2002; Kramer and Hall, 2005).

Previous reports have described the white-colored phenotype in PDS-silenced plants only on systemic leaves (Kumagai et al., 1995; Ruiz et al., 1998; Ratcliff et al., 2001) and VIGS efficacy reduced 28 d postinoculation for the potato virus X vector (Ratcliff et al., 2001). We repeated the experiments reported by Ruiz et al. (1998) and also observed the white-colored phenotype not only on systemic leaves, but, more precisely, on newly emerging systemic leaves. Because of the slow growth of orchids (more than 6 months to generate a new leaf for Phalaenopsis), no new leaves were able to generate before VIGS efficacy was reduced. Thus, PDS is not a suitable visual marker in VIGS of Phalaenopsis orchids because of the slow growth of the orchids. Therefore, we developed a control vector that targets the MADS-box gene family to induce visible morphological changes. The vector can be applied in VIGS of both colored and noncolored Phalaenopsis orchids. In addition, we also demonstrated that VIGS could be used to target family genes simultaneously, which might help in studies of family genes with redundant functions that are not easily analyzed by other genetic approaches.

The established CymMV-based vector was successful in knocking down the expression of *PeMADS6* specifically in all orchid floral organs. The knockdown levels varied in different floral organs, with at least 37% knockdown in sepals and up to 77% in lips. The knockdown level induced by VIGS might not have been enough to induce flower morphological change. MADS-box genes have been found to be dosage dependent and may require complete silencing to produce a phenotype (Zachgo et al., 1995; Scortecci et al., 2001; Yu et al., 2002).

Interestingly, the relative level of reduction of the *PeMADS6* level in pCymMV-pro60-PeMADS6-IR-inoculated plants varied among floral organs (Fig. 5, A and B). Differential silencing of *PeMADS6* in floral organs was related more to the accumulation of CymMV (Fig. 5C) than to the endogenous transcript levels of *PeMADS6* (Fig. 5D). One possible explanation is that differential transcription of MADS-box family genes changes the cellular condition in floral organs, thus leading to differential replication of CymMV.

The plants used in our analysis are tetraploid. Plants with multiploid genomes are common in commercial cultivars. Generally, loss-of-function assays are not easily performed in plants with multiploid genomes because T-DNA insertion or transposon tagging to target all the same genes residing in different chromosome locations is difficult. Applying VIGS to silence genes has been reported in multiploid plants, such as potato (*Solanum tuberosum*; Faivre-Rampant et al., 2004), wheat (*Triticum aestivum*; Scofield et al., 2005) and, here, *P. amabilis* var. *formosa* and *P.* Sogo Musadium.

VIGS efficacy is progressively reduced over time (Ratcliff et al., 2001). Our data with PDS used as a marker also show that VIGS efficacy was reduced after 8 weeks. Interestingly, in some of our MADS-box family gene-silencing plants, the initial buds were

Table II. *Ratio of affected plant organs in MADS-box gene-silenced plants*

	Initial Buds Abortion[a]	Flowers with Greenish Streaks/Patches[a]		
		Sepal	Petal	Lip
P. amabilis var. *formosa*				
Exp. 1	3/8[b] (8/46)[c]	8/8 (23/38)[d]	4/8 (8/38)[d]	2/8 (3/38)[d]
Exp. 2	2/6 (6/34)	5/6 (16/28)	2/6 (5/28)	1/6 (1/28)
Exp. 3	2/8 (10/50)	7/8 (25/40)	3/8 (10/40)	1/8 (2/40)
P. Sogo Musadium				
Exp. 1	3/3 (8/14)	3/3 (6/6)	3/3 (6/6)	3/3 (6/6)
Exp. 2	2/6 (6/37)	5/6 (23/31)	3/6 (12/31)	2/6 (7/31)

[a]Indicates the type of changes on plants (Exp.). [b]Number of affected plants to total number of inoculated plants. [c]Number of affected buds to total number of buds. [d]Number of affected flowers to total number of blossomed flowers.

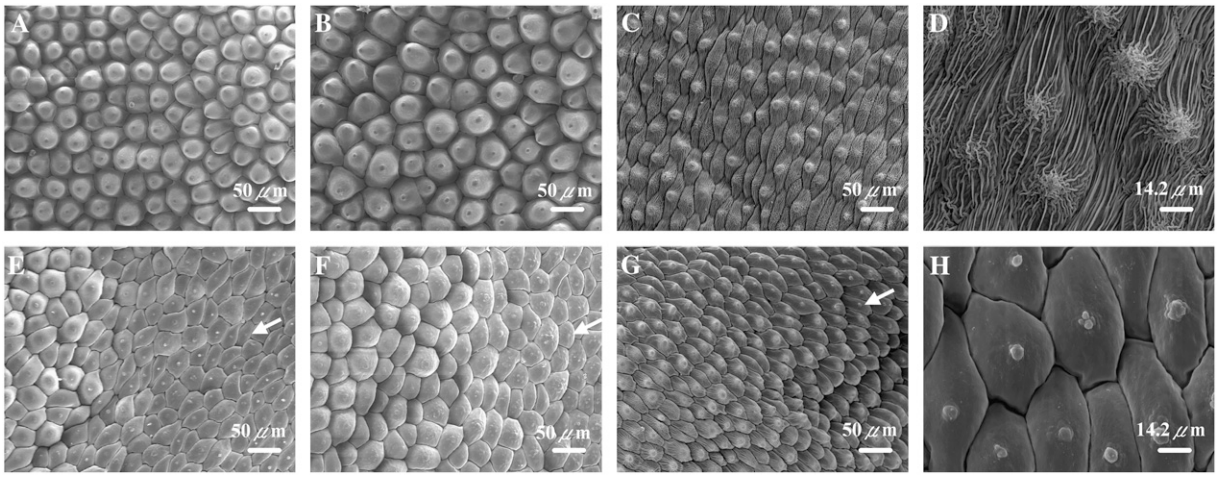

Figure 8. Scanning electron microscopy of epidermis of flowers. Epidermis of flowers of *P.* Sogo Musadium inoculated with buffer (A–D) and inoculated with transcripts of pCymMV-pro60-PeMADS6 (E–H) was examined by scanning electron microscope. Photos of adaxial (A and E) and abaxial (B and F) petal epidermis and adaxial lip epidermis (C, D, G, and H) are shown. A, B, C, E, F, and G are in 200× magnification; D and H are in 700× magnification. Arrows indicate greenish tissue of flower epidermis. Scale bars in micrometers (μm) are indicated.

aborted and later flowers were able to blossom on the upper stalks (Table II). This observation may be due to the MADS-box gene being reduced more prominently initially and the reduced levels reaching the threshold for flowers to fully develop and blossom; however, later, due to reduced gene-silencing efficacy and thus more elevated levels of MADS-box gene transcripts, flowers were able to develop further. We also found that more than 85% of the transcript levels of all three analyzed genes were reduced in initial flower buds, the reduced levels being more prominent in the initial flower buds (Fig. 9A) than in flowers (Fig. 9B). These results again suggest that VIGS efficacy was progressively reduced after some period.

Our in vivo experiment demonstrates an efficient way to study genes involved in the reproductive stage of plants with a long life cycle. The developed vectors will contribute well to functional genomics studies of orchids and similar strategies may be applied to the study of plants for which general conventional molecular and genetics approaches are unavailable.

MATERIALS AND METHODS

Plants

Phalaenopsis amabilis var. *formosa* and *Phalaenopsis* Sogo Musadium are both tetraploid commercial cultivars. *P. amabilis* var. *formosa* plants were obtained from the Taiwan Sugar Research Institute (Tainan, Taiwan), and *P.* Sogo Musadium plants were purchased from I-Hsin Biotechnology (Chiayi, Taiwan). Plants were kept in an insect-proof and thermal-controlled (20°C–28°C) greenhouse at the Department of Plant Pathology and Microbiology, National Taiwan University. RT-PCR with the primer pairs for odontoglossum ringspot

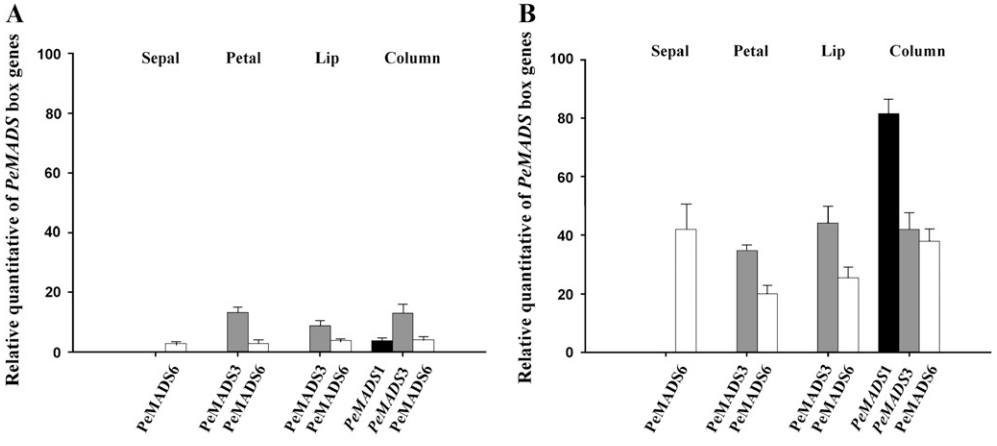

Figure 9. Relative quantification of MADS-box genes by real-time RT-PCR. Relative quantification of *PeMADS1*, *PeMADS3*, *PeMADS6*, and transcripts in flower buds (A) or flowers (B) of *P.* Sogo Musadium infected with pCymMV-pro60-PeMADS6. The mean *PeMADS1*, *PeMADS3*, and *PeMADS6* transcript level in flower buds or flowers of mock-inoculated plants was set to 100% for relative quantification of each gene.

Table III. *Primers designed for PCR or RT-PCR amplification and construction of recombinant CymMV*

Primer	Nucleotide Sequence
CyMV-5′[a]	5′-GCC**AATTAACCCTCACTAAA**GAAAA-CCAAACCTCACGTCTAATCCGCTATC-CGA-3′
CymMV-F3783	5′-ATTGCCTACAACGCCACCAGATACCA-3′
CymMV CP-F	5′-GAAATAATCATGGGAGAGCC-3′
CymMV CP-R	5′-AGTTTGGCGTTATTCAGTAGG-3′
CymMV-R3865	5′-AAGCTCTTCTTCTCAGGGCACACAT-3′
CymMV-*Spe*I[b]	5′-CGC*ACTAGT*TTTTTTTTTTTTTTTTTTTTT-TTTATTTATCTGGCTAAACTTAT-3′
CymMV-*Sma*I-F[c]	5′-CACTCCAACT*CCCGGG*AGCTGTCACT-TACTCCGC-3′
CymMV-*Sma*I-R[c]	5′-AGTAAGTGACAGCT*CCCGGG*AGTTG-GAGTGGGCTCT-3′
CymMV-pro-60	5′-GGGCTATTACTATCACTAACT-3′
CymMV-pro-100	5′-GGGAAATAAAGTAGCCATAGG-3′
ORSV CP-F	5′-ACGCACAATCTGATCCGTA-3′
ORSV CP-R	5′-ATCCGCAGTGAAAACCC-3′
GFP-F	5-GGATCCAAGGAGATATAACA-3′
GFP-R	5′-GAGCTCTTAAAGCTCATCA-3′
PeMADS1RT-F	5′-GAATGAACTGCTGCATGCTGA-3′
PeMADS1RT-R	5-GCTCATATGCTGATGCTGCTG-3′
PeMADS3 RT-F	5′AACTGCGTGGTCTTGAGCAAA-3′
PeMADS3 RT-R	5′-TTTCCAGCTCCCGGAGTAAGT-3′
PeMADS6-500-F	5′-GAGGGGGAAAGATAGAGAT-3′
PeMADS6-500-R	5′-ATTGGGCTGAATGGGTTG-3′
PeMADS6-150-F	5′-AGGGAGTATGAGAGAACTCGA-3′
PeMADS6-150-R	5′-CGGAATTCTTAAAAACCAGGAAAGC-AGT-3′
PeMADS6RT-F[d]	5′-GGCTCAATACTATTGCACCA-3′
PeMADS6RT-R[d]	5′-GGACACGAAAAGTCATTGGCA-3′
PeMADS6RT5-F[e]	5′-GGTTTTCGCTTCTGCTCCTGA-3′
PeMADS6RT5-R[e]	5′-TCACTTGCCGGTTGGTTGAGT-3′
PeMADS7 RT-F	5′-TGAGAGCATTCCAAGCTTCGA-3′
PeMADS7 RT-R	5′-TGCAGACTGATCGGCTTTTG-3′
CymMVRT-F	5′TGATGCTGGCCACTAACGATC-3′
CymMVRTR-R	5′-GGAATCAACGGCATCGAAGA-3′
Ubiqutin RT-F	5′-CCGGATCAGCAAAGGTTGA-3′
Ubiqutin RT-R	5′-AAGATTTGCATCCCTCCCC-3′
PDS-F	5′-ATCCAGATGGAGCTTTCTATGC-3′
PDS-R	5′-CCTCAGGTAAAAGAAGCTTCA-3′
PDS RT-F[f]	5′-CTATGCAAGCCGATTGTCGAA-3′
PDS RT-R	5′-CGTTGCTCAGCACAAATTGCT-3′

[a]T3 promoters are indicated by bold letters. [b]*Spe*I site is indicated by italic letters. [c]*Sma*I site is indicated by italic letters. [d]Used in pCymMV-pro60-PeMADS6-inoculated plants for real-time RT-PCR quantification to avoid amplification of *PeMADS6* inserted in vector. [e]Used in pCymMV-pro60-PeMADS6IR-inoculated plants for real-time RT-PCR quantification to avoid amplification of *PeMADS6* inserted in vector. [f]Used in pCymMV-pro60-PDS-inoculated plants for real-time RT-PCR quantification to avoid amplification of PDS inserted in vector.

virus (ORSV) CP-forward (F), ORSV CP-reverse (R), and CymMV CP-F, CymMV CP-R (Table III) was used for monthly detection of the two prevalent orchid viruses to ensure that the plants were virus free.

Virus Isolates

We selected healthy-looking plants with higher antibody detection values as analyzed by ELISA with the use of an antibody against CymMV. The selected plants were double checked on RT-PCR with the primer pairs for CymMV CP-F and CymMV CP-R (Table III) to confirm CymMV infection. CymMV was isolated from the infected plants by rubbing the sap extracted from the infected plant to *Cassia occidentals*, followed by three consecutive, single local lesion isolations. These isolates were rubbed to *P. amabilis* var. *formosa* and maintained in the greenhouse for at least 6 months. One symptomless CymMV isolate was selected for analysis.

Construction of Infectious Clones

All primers used in this study are listed in Table III. RNA was extracted from CymMV-infected plants and the primers for CymMV-R3865 and CymMV-*Spe*I were used to synthesize two cDNAs. Synthesized cDNAs were used as a template DNA and the primer pairs for CymMV-5′/CymMV-R3865 and CymMV-F3783/CymMV-*Spe*I were used in the PCR reaction to amplify two overlapping CymMV fragments. The first fragment contained nucleotides 1 to 3,865 with a T3 promoter and the second contained nucleotides 3,783 to 6,226, with a poly(A) tail and a *Spe*I site, respectively. Both fragments were cloned into pGEM-T (Promega) by incubating with DNA ligase (Promega) overnight at 4°C, and then transformed into *Eschericia coli*, DH5α, to construct pCymMV-1 and pCymMV-2, respectively. The two plasmids were digested with *Not*I and *Sna*I and then separated on 1% agarose gels. The 3.9- and 5.4-kb fragments derived from pCymMV-1 and pCymMV-2, respectively, were gel purified by use of the gel extraction kit (Qiagen). The purified fragments were ligated with T4 DNA ligase to construct the cDNA infectious clone pCymMV-M1 (Fig. 1).

Construction of CymMV Expression Vectors

pCymMV-M1 was used as the template and the primer pairs for CymMV-*Sma*I-F/CymMV-*Spe*I and CymMV-*Sma*I-R/CymMV-F3783 were used in the PCR reactions. The amplified fragments were gel purified and mixed together in a 1:1 ratio for PCR for five cycles and then the primer pair for CymMV-F3783/CymMV-*Spe*I was added for another 30 cycles. The amplified products were digested with *Nhe*I and *Hpa*I and separated on 1% agarose gels to purify the 1.3-kb fragment. pCymMV-M1 was also digested with *Nhe*I and *Hpa*I and separated on 1% agarose to purify the 8-kb fragment. The two digested fragments were ligated for the construction of pCymMV-*Sma*I. pCymMV-M1 was used as the template DNA, and the primer pairs for CymMV pro60/CymMV-*Spe*I and CymMV-pro100/CymMV-*Spe*I were used in the PCR reaction. The PCR-amplified products were digested with *Hpa*I and ligated to *Sma*I and *Hpa*I predigested pCymMV-*Sma*I to construct pCymMV-pro60 and pCymM-pro100, respectively. pBIN-gfp-5-ER (containing the GFP gene; distributed by Dr. Jim Haseloff, GenBank accession no. U87974 [Siemering et al., 1996]) was used as the template DNA, and the primer pairs for GFP-F and GFP-R were used in the PCR reaction. The amplified fragments were ligated to *Sma*I-digested pCymMV-pro60 and pCymMV-pro100 to construct pCymMV-pro60-GFP and pCymMV-pro100-GFP, respectively.

The primer pairs for PeMADS6-150-F/PeMADS6-150-R, and template DNA of pPeMADS6 (Tsai et al., 2005) were used to amplify the 150-nucleotide region (corresponding to 172–221 codons of *PeMADS6* open reading frame with the *Eco*RI site at the 3′ end). The amplified fragments were gel purified as described above and ligated to *Sma*I-digested pCymMV-pro60 to construct pCymMV-pro60-PeMADS6IR. The primer pairs for PDS-F and PDS-R and template nucleic acid extracted from *P. amabilis* var. *formosa* were used to amplify a 300-nucleotide PDS fragment. The amplified fragments were cloned into pCymMV-pro60 to create pCymMV-pro60-PDS. All PCR-amplified fragments have been sequenced completely.

RNA Extraction and Northern-Blot Hybridization

RNA used in northern-blot analysis and RT-PCR was extracted from plants as described (Tian et al., 1996). T7 RNA polymerase and *Hpa*I-digested pCymMV-M1 plasmids (corresponding to the 590 nucleotide of CymMV at its 3′ end) were used to generate negative-sense digoxigenin (DIG)-labeled probes (Roche Applied Science). Northern-blot hybridization was performed as described (Klaassen et al., 1996) and hybridization signals were detected by using the chemiluminescent substrate CDP *STAR* (Roche Applied Science) and exposing blots to Fuji medical x-ray film (Fuji).

RT-PCR

RNA extracted from CymMV-infected plants was used as a template for synthesis of cDNAs by Moloney murine leukemia virus reverse transcriptase following the manufacturer's instructions (Promega). PCR amplification

conditions were as described (Rubio et al., 2000). cDNAs were PCR amplified in a mixture containing 1.5 mM $MgCl_2$, 1 mM of each of the four deoxynucleotide triphosphates, 2.5 units of Taq DNA polymerase (Promega), and 50 ng of each oligonucleotide. PCR cycles were at 94°C for 4 min for 1 cycle, then 94°C for 30 s, 55°C for 30 s, and 72°C for 1 min for 30 cycles, followed by an extension step at 72°C for 10 min.

In Vitro Transcription

Capped transcripts corresponding to the wild-type virus and the constructed vectors of CymMV were synthesized as described (Rubio et al., 2000; Yeh et al., 2000), except that pCymMV-M1 and its derivative plasmids were linearized with *Spe*I.

Real-Time Quantitative RT-PCR

Total RNA extracted from plant tissue (0.2 g) was as described (Chang et al., 1993) and dissolved in 50 μL diethyl pyrocarbonate-treated water. RNA was treated with RNase-free DNase (Ambion) to remove residual DNA. A one-tenth aliquot of RNA was used as a template for synthesis of cDNAs on Moloney murine leukemia virus-reverse transcriptase following the manufacturer's instructions (Promega). A one-fourth aliquot of the cDNA was used as a template with 2× SYBR Green PCR master mix (Applied Biosystems) for quantitative PCR in an ABI Prism 7000 sequence detection system following the manufacturer's instructions (Applied Biosystems). The primers used in quantification are listed in Table III. For gene quantification, samples (0.2 g) were collected from three randomly selected plants. For each real-time RT-PCR reaction, each sample was analyzed in triplicate. The relative quantification was calculated according to the manufacturer's instructions (Applied Biosystems). The *ubiqutin10* gene was used as an internal quantification control. Real-time RT-PCR was performed in each repeated experiment.

Detection of siRNA

siRNA was detected as reported (Hamilton and Baulcombe, 1999) with modifications. Total RNA was extracted as described (Chang et al., 1993), except that a one-tenth (v/v) volume of 3 M sodium acetate, pH 5.2, was used to precipitate total nucleic acids. Prehybridization and hybridization were performed at 35°C. CymMV siRNA was detected with use of the DIG-labeled antisense CymMV 3′ end (corresponding to 5,636–6,226 nucleotides of CymMV genomic RNA) RNA probes (DIG northern starter kit; Roche). *PeMADS6* siRNA was detected by use of a PCR-amplified, DIG-labeled *PeMADS6* fragment (amplified with the primer pair PeMADS6-500F and PeMADS6-150R, and the template DNA of pPeMADS6).

Sequence data from this article have been deposited with the EMBL/GenBank data libraries under accession numbers *PeMADS1*, AF234617; *PeMADS2*, AY378149; *PeMADS3*, AY378150; *PeMADS4*, AY378147; *PeMADS5*, AY378148; and *PeMADS6*, AY678299.

ACKNOWLEDGMENTS

We thank Dr. Tongyan Tian for helpful discussion and Laura Heraty for help with manuscript editing. We also thank the Taiwan Sugar Research Institute and I-Hsin Biotechnology for taking care of plant materials.

Received November 7, 2006; accepted November 29, 2006; published December 22, 2006.

LITERATURE CITED

Babbitt C, Giorgianni M, Price A (2002) Evo-devo comes into focus. Bioessays **24:** 677–679

Benedito VA, Visser PB, Angenent GC, Krens FA (2004) The potential of virus-induced gene silencing for speeding up functional characterization of plant genes. Genet Mol Res **3:** 323–341

Brigneti G, Martin-Hernandez AM, Jin H, Chen J, Baulcombe DC, Baker B, Jones JD (2004) Virus-induced gene silencing in Solanum species. Plant J **39:** 264–272

Burch-Smith TM, Anderson JC, Martin GB, Dinesh-Kumar SP (2004) Applications and advantages of virus-induced gene silencing for gene function studies in plants. Plant J **39:** 734–746

Burch-Smith TM, Schiff M, Liu Y, Dinesh-Kumar SP (2006) Efficient virus-induced gene silencing in Arabidopsis. Plant Physiol **142:** 21–27

Chang S, Puryear J, Cairney J (1993) A simple and efficient method for isolating RNA from pine trees. Plant Mol Biol Rep **155:** 113–116

Chapman S, Kavanagh T, Baulcombe DC (1992) *Potato virus X* as a vector for gene expression in plants. Plant J **2:** 549–557

Chen WH, Kao YY, Lin TY, Chen CC, Wu WL, Chen HH (2001) Genomic Study of *Phalaenopsis* Orchid. Proceedings of APOC7, Nagoya, Japan

Constantin GD, Krath BN, MacFarlane SA, Nicolaisen M, Johansen IE, Lund OS (2004) Virus-induced gene silencing as a tool for functional genomics in a legume species. Plant J **40:** 622–631

Costa MM, Fox S, Hanna AI, Baxter C, Coen E (2005) Evolution of regulatory interactions controlling floral asymmetry. Development **132:** 5093–5101

Dressler RL (1993) Phylogeny and Classification of the Orchid Family. Dioscorides Press, Portland, OR

Faivre-Rampant O, Gilroy EM, Hrubikova K, Hein I, Millam S, Loake GJ, Birch P, Taylor M, Lacomme C (2004) Potato virus X-induced gene silencing in leaves and tubers of potato. Plant Physiol **134:** 1308–1316

Fofana IB, Sangare A, Collier R, Taylor C, Fauquet CM (2004) A geminivirus-induced gene silencing system for gene function validation in cassava. Plant Mol Biol **56:** 613–624

Gewin V (2005) Functional genomics thickens the biological plot. PLoS Biol **3:** e219

Gorden B (1998) *Phalaenopsis* flower induction (or, how to make them bloom). Am Orchid Soc Bull **9:** 908–910

Hamilton AJ, Baulcombe DC (1999) A species of small antisense RNA in posttranscriptional gene silencing in plants. Science **286:** 950–952

Hileman LC, Drea S, Martino G, Litt A, Irish VF (2005) Virus-induced gene silencing is an effective tool for assaying gene function in the basal eudicot species Papaver somniferum (opium poppy). Plant J **44:** 334–341

Holzberg S, Brosio P, Gross C, Pogue GP (2002) Barley stripe mosaic virus-induced gene silencing in a monocot plant. Plant J **30:** 315–327

Katou S, Yoshioka H, Kawakita K, Rowland O, Jones JD, Mori H, Doke N (2005) Involvement of PPS3 phosphorylated by elicitor-responsive mitogen-activated protein kinases in the regulation of plant cell death. Plant Physiol **139:** 1914–1926

Klaassen VA, Mayhew D, Fisher D, Falk BW (1996) In vitro transcripts from cloned cDNAs of the lettuce infectious yellows closterovirus bipartite genomic RNAs are competent for replication in Nicotiana benthamiana protoplasts. Virology **222:** 169–175

Kramer EM, Hall JC (2005) Evolutionary dynamics of genes controlling floral development. Curr Opin Plant Biol **8:** 13–18

Kumagai MH, Donson J, della-Cioppa G, Harvey D, Hanley K, Grill LK (1995) Cytoplasmic inhibition of carotenoid biosynthesis with virus-derived RNA. Proc Natl Acad Sci USA **92:** 1679–1683

Lin S, Lee HC, Chen WH, Chen CC, Kao YY, Fu YM, Chen YH, Lin TY (2001) Nuclear DNA contents of *Phalaenopsis sp.* and *Doritis pulcherrima.* J Am Soc Hortic Sci **126:** 195–199

Marathe R, Anandalakshmi R, Smith TH, Pruss GJ, Vance VB (2000) RNA viruses as inducers, suppressors and targets of post-transcriptional gene silencing. Plant Mol Biol **43:** 295–306

Pennisi E (2004) Evolution of developmental diversity meeting. RNAi takes Evo-Devo world by storm. Science **304:** 384

Ratcliff F, Martin-Hernandez AM, Baulcombe DC (2001) Technical advance: tobacco rattle virus as a vector for analysis of gene function by silencing. Plant J **25:** 237–245

Robertson D (2004) VIGS vectors for gene silencing: many targets, many tools. Annu Rev Plant Biol **55:** 495–519

Rubio L, Yeh HH, Tian T, Falk BW (2000) A heterogeneous population of defective RNAs is associated with lettuce infectious yellows virus. Virology **271:** 205–212

Ruiz MT, Voinnet O, Baulcombe DC (1998) Initiation and maintenance of virus-induced gene silencing. Plant Cell **10:** 937–946

Scofield SR, Huang L, Brandt AS, Gill BS (2005) Development of a virus-induced gene-silencing system for hexaploid wheat and its use in functional analysis of the Lr21-mediated leaf rust resistance pathway. Plant Physiol **138:** 2165–2173

Scortecci KC, Michaels SD, Amasino RM (2001) Identification of a MADS-box gene, FLOWERING LOCUS M, that represses flowering. Plant J **26:** 229–236

Shivprasad S, Pogue GP, Lewandowski DJ, Hidalgo J, Donson J, Grill LK, Dawson WO (1999) Heterologous sequences greatly affect foreign gene expression in tobacco mosaic virus-based vectors. Virology **255:** 312–323

Siemering KR, Golbik R, Sever R, Haseloff J (1996) Mutations that suppress the thermosensitivity of green fluorescent protein. Curr Biol **6:** 1653–1663

Smith NA, Singh SP, Wang MB, Stoutjesdijk PA, Green AG, Waterhouse PM (2000) Total silencing by intron-spliced hairpin RNAs. Nature **407:** 319–320

Tian T, Klaassen VA, Soong J, Wisler G, Duffus JE, Falk BW (1996) Generation of cDNAs specific to *Lettuce infectious yellows closterovirus* and other whitefly-transmitted viruses by RT-PCR and degenerate oligonucleotide primers corresponding to the *closterovirus* gene encoding the heat shock protein 70 homolog. Phytopathology **86:** 1167–1173

Tsai WC, Hsiao YY, Lee SH, Tung CW, Wang DP, Wang HC, Chen WH, Chen HH (2006) Expression analysis of the ESTs derived from the flower buds of *Phalaenopsis equestris*. Plant Sci **170:** 426–432

Tsai WC, Kuoh CS, Chuang MH, Chen WH, Chen HH (2004) Four *DEF*-like MADS box genes displayed distinct floral morphogenetic roles in *Phalaenopsis* orchid. Plant Cell Physiol **45:** 831–844

Tsai WC, Lee PF, Chen HI, Hsiao YY, Wei WJ, Pan ZJ, Chuang MH, Kuoh CS, Chen WH, Chen HH (2005) *PeMADS6*, a *GLOBOSA/PISTILLATA*-like gene in *Phalaenopsis equestris* involved in petaloid formation, and correlated with flower longevity and ovary development. Plant Cell Physiol **46:** 1125–1139

Valentine T, Shaw J, Blok VC, Phillips MS, Oparka KJ, Lacomme C (2004) Efficient virus-induced gene silencing in roots using a modified tobacco rattle virus vector. Plant Physiol **136:** 3999–4009

Wang MB, Waterhouse PM (2002) Application of gene silencing in plants. Curr Opin Plant Biol **5:** 146–150

Wesley SV, Helliwell CA, Smith NA, Wang MB, Rouse DT, Liu Q, Gooding PS, Singh SP, Abbott D, Stoutjesdijk PA, et al (2001) Construct design for efficient, effective and high-throughput gene silencing in plants. Plant J **27:** 581–590

Yeh HH, Tian T, Rubio L, Crawford B, Falk BW (2000) Asynchronous accumulation of lettuce infectious yellows virus RNAs 1 and 2 and identification of an RNA 1 trans enhancer of RNA 2 accumulation. J Virol **74:** 5762–5768

Yu H, Xu Y, Tan EL, Kumar PP (2002) AGAMOUS-LIKE 24, a dosage-dependent mediator of the flowering signals. Proc Natl Acad Sci USA **99:** 16336–16341

Zachgo S, Silva Ede A, Motte P, Trobner W, Saedler H, Schwarz-Sommer Z (1995) Functional analysis of the Antirrhinum floral homeotic DEFICIENS gene in vivo and in vitro by using a temperature-sensitive mutant. Development **121:** 2861–2875

Zhang C, Ghabrial SA (2006) Development of bean pod mottle virus-based vectors for stable protein expression and sequence-specific virus-induced gene silencing in soybean. Virology **344:** 401–411